ANALYTICAL STUDY OF ELECTRONIC AND OPTICAL PROPERTIES OF InAs / InGaAs QUANTUM DOT LASER

Soufyane TALEB[1*], Belabbéss SOUDINI[1], Ibrahim LAGRAA[1]

[1] Applied Materials Laboratory (AML), University of Sidi Bel Abbès, Sidi Bel Abbès, Algeria.

ABSTRACT

As part of improving the properties of optoelectronic components, by a better quantum confinement of electrons and holes, we carried out an analytical study of carrier dynamics in quantum dots lasers (QDL). Our calculations are performed on the set of five rate equations for carriers and photons in two energy states. The results of the curriers density, photon density, output power, and the in /out scattering rates between the quantum dot (QD) and quantum well (QW) versus the time and the injection current. Our results are in agreement with others work and then a confirmation of the validity of this numerical model to reproduce the electronic and the optical properties of quantum dot laser.

Keywords: laser semiconductor; quantum dot; InAs / InGaAs; rate equations model.

Soufyane TALEB:talebs2011@hotmail.fr

1. INTRODUCTION

Quantum dot (QD) is a semiconductor-based compound of which the excitons are confined in the three dimensions of space, which induces a finer state density than in conventional structures. This confinement gives the quantum dots properties similar to those of an atom, for this quantum dots are sometimes described as artificial. Quantum dot lasers have attracted much attention in recent years [1– 3] because they have excellent properties such as threshold current, temperature stability, chirp, and feedback Insensitivity [4–6].

In this paper, InAs/InGaAs QDs are considered as active medium in a QD laser consisting of several energy levels for confined carriers. It is assumed that all the QDs are uniform and have the same size and shape. Thus, the homogeneous broadening effect is ignored according to the theoretical and experimental studies performed in references [7]. The QDs are integrated in a two-dimensional QW acting as a carrier reservoir, the structure of the band is represented in the Fig.1., the numerical model used for InAs/InGaAs QD laser is based on the set of coupled rate equations, which consists of two energy levels of which are join in lasing,

a) **b)**

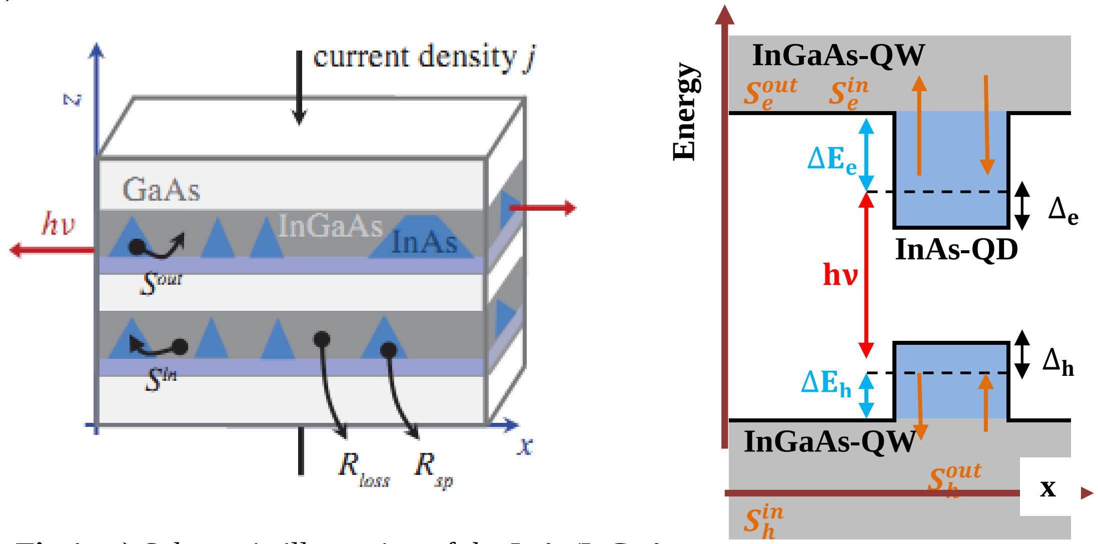

Fig.1. a) Schematic illustration of the InAs/InGaAs QD laser. b) Energy diagram of the band structure across a QD. hν labels the ground state (GS) lasing energy. ΔE_e and ΔE_h mark the distance of the GS from the QW band edge for electrons and holes, respectively. Δ_e and Δ_h denote the distance to the bottom of the QD.

In this work we used the 4th order of Runge-Kutta method in MATLAB software, for the extraction time variation of electron, hole and photon density, The Coulomb scattering rates for electrons and holes, output power in the QD for different injection current and modulation response of the photon density.

2. THEORETICAL MODEL

The QD laser numerical model based on the five of coupled rate equations (REs), through an analysis of carrier dynamic inside the QD. The model is divided into four carrier populations: The population densities of electrons in the QD (n_e) and QW (W_e), and the population densities of holes in the QD (n_h) and QW (W_h), a fifth population density of the emitted photons in the longitudinal direction (n_{ph}). The rate equation system can be written as follow:

$\frac{dn_e}{dt} = -\frac{1}{\tau_e} n_e + S_e^{in} N^{QD} - R_{ind}(n_e, n_h) - R_{sp}(n_e, n_h),$

(1)

$\frac{dn_h}{dt} = -\frac{1}{\tau_h} n_h + S_h^{in} N^{QD} - R_{ind}(n_e, n_h) - R_{sp}(n_e, n_h),$

(2) $\frac{dW_e}{dt} = \frac{j(t)}{e_0} + \frac{n_e}{\tau_e} \frac{N^{WL}}{N^{QD}} - S_e^{in} N^{WL} - \widetilde{R}_{sp}(W_e, W_h),$

(3) $\frac{dW_h}{dt} = \frac{j(t)}{e_0} + \frac{n_h}{\tau_h} \frac{N^{WL}}{N^{QD}} - S_h^{in} N^{WL} - \widetilde{R}_{sp}(W_e, W_h),$

(4) $\frac{dn_{ph}}{dt} = -2\, k\, n_{ph} + \Gamma R_{ind}(n_e, n_h) + \beta R_{sp}(n_e, n_h),$

(5)

The nonlinear rate equations (1)–(5) show the dynamics of the charge carrier densities in the QDs (n_e and n_h), the carrier densities in the QW (W_e and W_h)(e and h are electrons and holes, respectively), and the photon density n_{ph}. R_{ind} is the rate for the induced processes of absorption and emission and writes as follows:

$$R_{ind}(n_e, n_h, n_{ph}) = WA(n_e + n_h - N^{QD})n_{ph} \quad (6)$$

where N^{QD} denotes twice the QD density taking into account the spin degeneracy, W is the Einstein coefficient, and A is the WL normalization area the ridge waveguide QD laser used here has a lateral ridge dimension of A =4 um x 1mm). The second types of terms in the first four equations are the rates for the radiative processes. There are rates for the spontaneous emissions in the QD and WL, respectively:

$$R_{sp}(n_e, n_h) = \frac{W}{N^{QD}} n_e n_h \quad (7)$$

$$\tilde{R}_{sp}(W_e, W_h) = \frac{W}{N^{WL}} W_e W_h \quad (8)$$

with a WL effective density of states N^{WL}=1x10^{17} m^{-2}. Both spontaneous emission and induced processes are proportional to the Einstein coefficient [8], $w = |\mu|^2/3\pi\mathcal{E}_0\hbar\,(\omega/c/\sqrt{\mathcal{E}_{bg}})^3$ where μ is the dipole moment, $\mathcal{E}_0$is the vacuum permittivity, $\hbar$ is Planck's reduced constant, ω is the frequency, c is the speed of light and $\mathcal{E}_{bg}$ is the background dielectric constant. The optical confinement factor is given by $\Gamma = N^{QD} a_L \gamma_{xy} \Gamma_z$, where Γ_z is the vertical confinement factor, $a_L$the number of QD layers, and γ_{xy} the in-plane size of a QD. β is the probability that the spontaneous emission, $j(t)$ is the injection current density, e_0 is the electronic charge. The coefficient $k = \left(k_{int} - \frac{\ln(r_1 r_2)}{2L}\right)\frac{c}{\sqrt{\varepsilon_{bg}}}$ expresses the total cavity loss [9], where L is the cavity length, and r_1, r_2 are the facet reflectivities and k_{int} are the internal losses [10]. Through the experimental details given in Ref [7] is taken $k = 0.12 ps^{-1}$. The carrier lifetimes τ_e and τ_h that result from Coulomb scattering between QDs and QW are defined by the nonlinear scattering rates as

$$\tau_e = (S_e^{in} + S_e^{out})^{-1} \tag{9}$$

$$\tau_h = (S_h^{in} + S_h^{out})^{-1} \tag{10}$$

Where S_e^{in} and S_h^{in} are the scattering rates from the WL to the QD for electrons and holes, respectively. Likewise S_e^{out} and S_h^{out} are the scattering rates from the QD to the WL.

Symbol	Value	Symbol	Value
r_1, r_2	0.32	m_e	$0.043\ m_0$
k_{int}	$220\ m^{-1}$	m_h	$0.45\ m_0$
L	1.10^{-3} m	ΔE_e	210 mev
c	3.10^{8} m/s	Δ_e	64 mev
ε_{bg}	13.18	ΔE_h	50 mev
Γ	0.001	Δ_h	6 mev
N^{QD}	$1.10^{14}\ m^{-2}$	μ	$0.75 e_0$ nm
N^{WL}	$1.10^{17}\ m^{-2}$	A	$4.10^{-9}\ m^2$
W	$0.7.10^{-9}\ s^{-1}$	β	5.10^{-6}

Figure I.1

Figure I.2 *Table 1: Numerical parameters used in the simulation [10].*

3. RESULTS AND DISCUSSION

a) **b)**

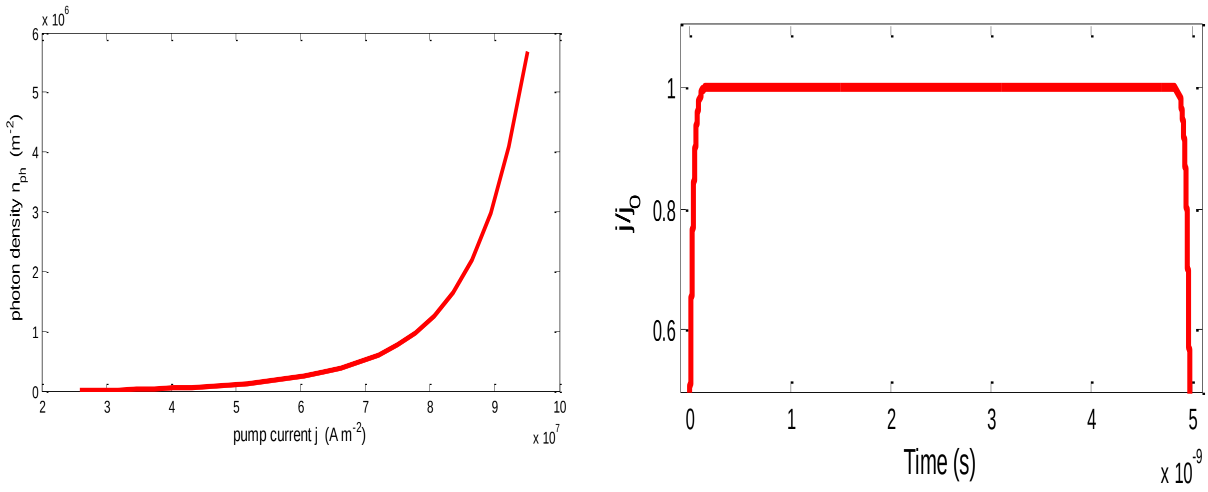

Fig.2. a)Simulated photon density n_{ph} vs injection current density j, b) Injection current pulse used in the simulations of turn-on characteristics.

The simulation of the rate equation system in MatLab enables a detailed theoretical study of the turn on characteristics and behavior of the QD laser until steady-state has been reached. In steady-state the laser emits photons at a constant rate which also means that the electron/hole transitions are unchanging in time. Fig. 2.a. Shows simulated photon density n_{ph} vs injection current density j, we can calculate The threshold current density j_{th}, which refers to the minimum current density necessary for lasing. Bay the extrapolated laser onset if spontaneous emission is neglected. Fig.2.b. represents the simulation a current pulse during turn-on and turn-off with a rise and fall time of 100 ps. The function of the current density is $j(t) = j_0 exp\left[-\left(\frac{t-2.5\ 10^{-9}}{2.49\ 10^{-9}}\right)^{90}\right]$ where j_0 denotes the maximum current density.

a) **b)**

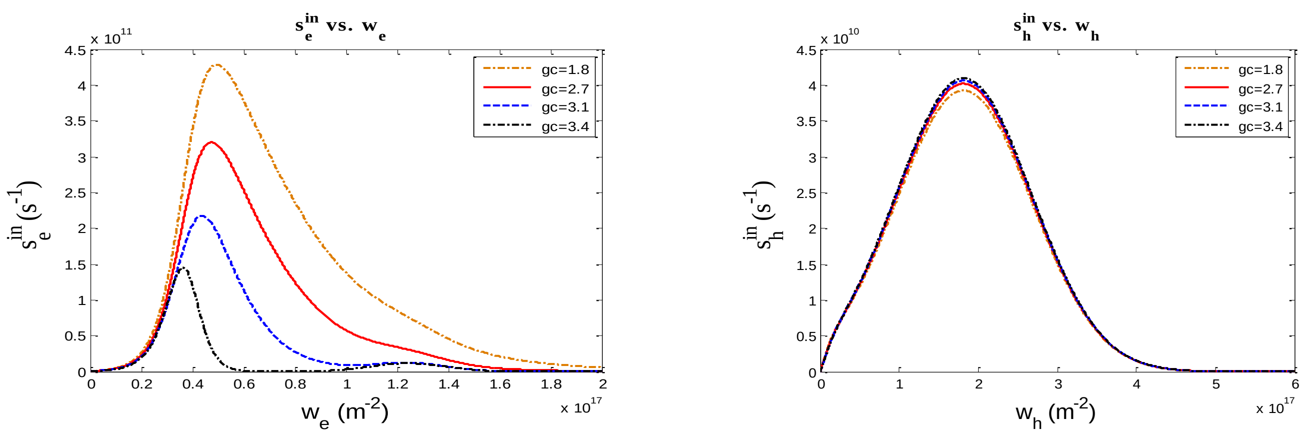

c) **d)**

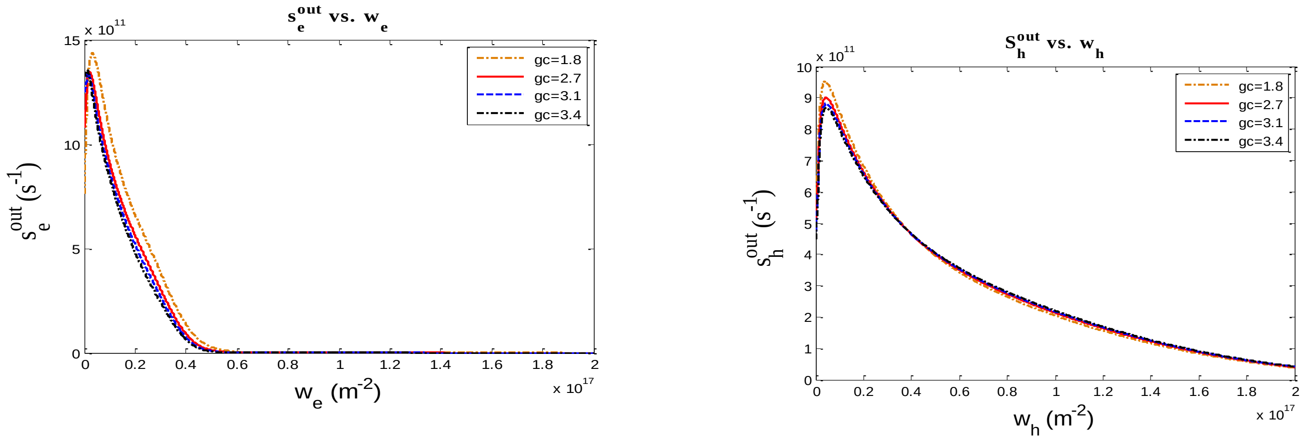

Fig.3. Coulomb scattering rates: a) S_e^{in}, b) S_h^{in}, c) S_e^{out}, d) S_h^{out} electrons and holes vs carrier density in the WL (W_e, W_h) calculated within the orthogonalized-plane-wave approach for different g_c ($g_c = \frac{W_e}{W_h}$).

Fig.3. shows the Coulomb scattering rates for electron and hole capture processes as a function of the respective WL electron and hole densities for different ratio g_c ($g_c = \frac{W_e}{W_h}$). The Coulomb scattering rates are larger for increasing WL carrier densities W_m (m=e, h) due to the increase of available scattering partners. The Pauli Exclusion Principle, however, stops the increase of the out-scattering for higher W_m resulting in a maximum of S_b^{out}.

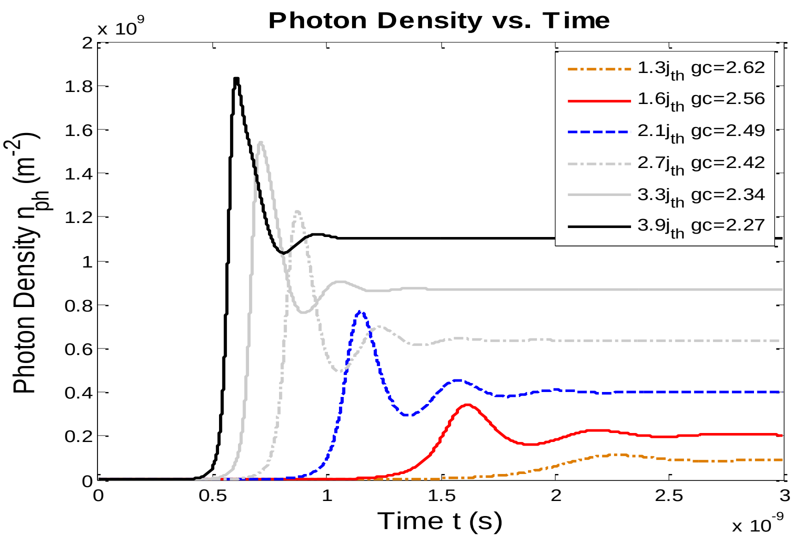

Fig.4. Photon density output from QD laser during turn-on with dynamic scattering rates for sex different pump currents.

Fig.4. show the simulated turn-on photon emission curves for different pump currents with dynamic scattering rates, the curve shows that the higher the current, the greater the number of electrons and holes feeding the system in a short period of time, thus forcing the system to commence emissions at a faster time. By comparing all the graphs, we observe that before the stability is reached, there is a strong damped relaxation oscillation, and he increases his speed by increasing the current. This is exactly the case with output power changes which are rep-

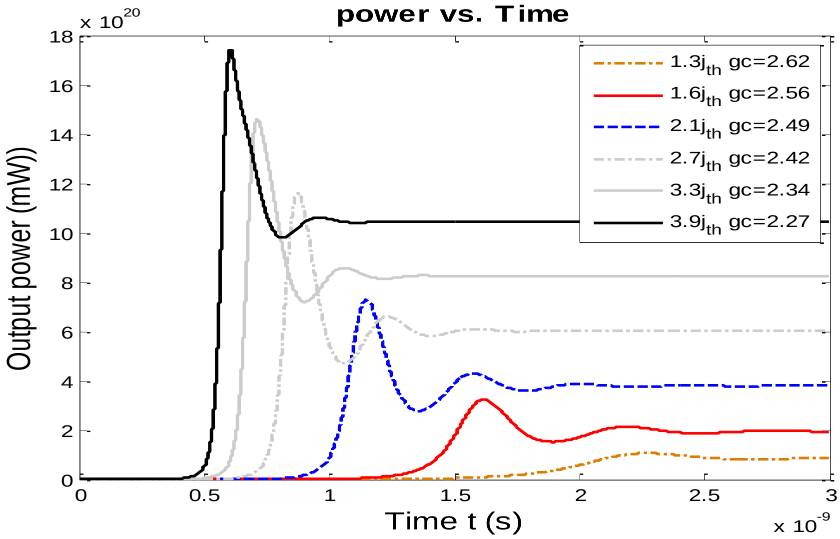

Fig.5. the temporal variation of output power for different injection current densities.

resented in Fig.5., which shows the effect of the intensity of the current on the power provided by this structure. Generally, by increasing the pump current, the photon density increases and hence the emission energy, this is due to the fact that radiative transition processes increase when more carriers are present in the system.

CONCLUSION

In this paper, the internal mechanism of the QD laser InAs/ InGaAs has been modeled and simulated, based on all five rate equations coupled to the carrier densities and photons, which exhibit the carrier dynamics in two levels energy, including GS and WL states. The simulation is carried out by using the 4th order of Runge-Kutta method in MATLAB software. To find out properties of quantum dot laser based InAs/InGaAs, we studied time variation of the photon densities, PI characteristic and the intensity modulation response. Our results are in agreement with other work and then a confirmation of the validity of this numerical model to reproduce the electronic and optical properties of the quantum dot laser. Finally, we can say that the results obtained in this work show interesting properties for InAs / InGaAs based on quantum dot lasers.

REFERENCE

[1] Rafailov, E. U., M. A. Cataluna, and E. A. Avrutin, Ultrafast Lasers Based on Quantum Dot Structures: Physics and Devices, Wiley, New York, (2011).

[2] Sugawara, M., R. K. Willardson, and E. R.Weber, Self-Assembled InGaAs/GaAs Quantum Dots (Semiconductors and Semimetals), Academic Press, (1999).

[3] Gioannini, M., A. Sevega, and I. Montrosset, "Simulations of differential gain and linewidth enhancement factor of quantum dot semiconductor lasers," Opt. Quantum Electron., Vol. 38, No. 4, 381-394, (2006).

[4] D. Bimberg, M. Grundmann, and N. N. Ledentsov, Quantum Dot Heterostructures Wiley, New York, (1999).

[5] D. Bimberg, M. Kuntz, and M. Lämmlin, Appl. Phys. A 80,1179 (2005).

[6] D. Bimberg, Electron. Lett. 44, 168 (2008).

[7] M. Kuntz, Ph.D. thesis, Technische Universität Berlin, (2006).

[8] E. Malić , M. J. P. Bormann, P. Hövel, M. Kuntz, D. Bimberg, A. Knorr, and E. Schöll, IEEE J. Sel. Top. Quantum Electron. 13, 1242 (2007).

[9] J. Gomis-Bresco, S. Dommers, V. V. Temnov, U. Woggon, M. Lämmlin, D. Bimberg, E. Mali´c, M. Richter, E. Schöll, and A. Knorr, "Impact of Coulomb scattering on the ultrafast gain recovery in InGaAs quantum dots," Phys. Rev. Lett., vol. 101, no. 25, pp. 256803-1 256803-4, Dec. (2008).

[10] K. Lüdge, M. J. P. Bormann, E. Mali´c, P. Hövel, M. Kuntz, D. Bimberg, A. Knorr, and E. Schöll, "Turn-on dynamics and modulation response in semiconductor quantum dot lasers," Phys.Rev.B, vol. 78, no. 3, pp. 035316-1–035316-11, (2008).